Journal of Nonlinear Modeling and Analysis
Volume 8, Number 2, April 2026, 405–430
https://global-sci.com/jnma
DOI:10.12150/jnma.2026.405

Dynamical Analysis of Virulence Evolution in Multistrain Infection Model Within Hosts

Yayuan Lei[1] and Gang Huang[1,†]

Received 21 January 2025; Accepted 16 July 2025

Abstract Understanding the evolutionary patterns of viral virulence characteristics from a microscopic perspective is crucial for effectively combating viral mutations. This paper investigates the dynamics of virulence trait development within healthy cells following pathogen invasion using adaptive dynamics, building on a viral dynamics model that accounts for multiple infectious strains within hosts. Ignoring viral evolution, stability analysis of equilibria reveals the competitive exclusion principle. When viral virulence evolves, we assume that the infection rate of healthy cells and the mortality rate of infected cells are functions of virulence. We establish global stability conditions for the system and examine the evolutionary trajectory of viral virulence using adaptive dynamics. Our results indicate that mutant viruses can cause trait substitution. The evolutionary singular strategy is identified as a continuously stable strategy without producing evolutionary branching. Furthermore, we consider the influence of certain parameters in the system on the evolution of singular strategies.

Keywords Viral infection model, adaptive dynamics, evolutionary singular strategy, stability analysis

MSC(2010) 92D30, 92D15, 34D20, 37N25.

1. Introduction

Over the past few decades, extensive research has been conducted on the evolution of virulence using a theoretical framework grounded in the principles of natural selection. This framework not only explains the varying levels of virulence observed in host-parasite interactions but also offers opportunities for effectively managing virulence to control disease spread. Furthermore, this evolutionary perspective elucidates the extent to which infectious agents contribute to the development of chronic illnesses and identifies diseases that can be prevented or treated through disease-control strategies such as vaccines and antibiotics.

The majority of recent theories that endeavor to elucidate the evolutionary mechanisms of parasites posit an association between virulence and transmission, commonly referred to as the "virulence-transmission trade-off" [2]. However, this

†the corresponding author.
Email address: huanggang@cug.edu.cn(G. Huang)
[1]School of Mathematics and Physics, China University of Geosciences, Wuhan 430074, China

concept has been met with significant controversy. To gain a comprehensive understanding of the ongoing debates in this field, it is crucial to recognize that the evolution of virulence had been studied extensively prior to the formulation of the trade-off hypothesis.

The presence of strain-specific virulence and the ability to convert one strain into another were highlighted in the attenuation of the anthrax bacillus. Then, evolutionary theories emerged to elucidate the mechanisms driving parasite virulence. Subsequently, research into viral strain virulence gained momentum. In nature, the interactions between hosts and pathogens are ubiquitous, leading hosts to develop a variety of defense mechanisms in response to pathogenic challenges [4,6–8,10,11,32,38,41]. In addition, during viral infection, the dynamics within the host can be analyzed using mathematical models [25]. Taking the human immunodeficiency virus (HIV) as an example, its unique intra-host dynamics distinguish it from other viral infections. One key feature is HIV's high degree of genetic variability, which results from its rapid replication and mutation rates. This genetic diversity poses significant challenges for both the immune system and antiviral therapies in completely eradicating the virus. Understanding these intra-host dynamics is crucial for developing effective treatment strategies, as the genetic diversity of HIV complicates efforts to find a cure for the infection.

What factors contribute to the variability in disease progression? Several key factors have been identified, including the virus's reproductive capacity, the immune system's proliferative ability, and the accelerated degradation of $CD4^+T$ cells caused by HIV [1, 3, 14, 17, 23, 24, 40]. Since the early 1990s, the predominant explanations for HIV's evasion of the immune response and subsequent immune system failure have centered on its evolutionary capabilities [9, 26, 27, 35, 36]. While all viruses can undergo evolutionary changes, HIV is recognized as the most rapidly evolving organism, generating multiple novel variants daily within a single host [18, 24, 33, 39]. This rapid evolution and extensive viral diversity can be attributed to several virus-specific factors. These include an exceptionally rapid reproduction cycle, producing approximately $10^{10} \sim 10^{12}$ new virions per patient per day [37], and an exceedingly high mutation rate of about 3×10^5 mutations per nucleotide base per replication cycle.

The extremely rapid rate of evolution has led to the emergence of drug-resistant strains [12] and significantly hindered the development of an efficacious vaccine [9]. The gradual increase in viral load during the asymptomatic stage can be attributed to evolutionary processes, where organisms adapt to enhance their fitness, particularly in terms of viral reproductive capacity [22]. As a result, the viral load increases proportionally with improvements in its reproductive potential.

There has been a significant increase in the application of mathematical models to investigate viral evolution at both population and within-host levels. This advancement has been facilitated by integrating within-host viral dynamics with between-host transmission dynamics. Most researchers have incorporated within-host models into epidemiological frameworks by introducing transmission rates that depend on viral load or disease-induced mortality [13, 16, 21, 42]. Additionally, it is commonly assumed that higher viral loads within hosts lead to increased parasite virulence, which in turn correlates with elevated transmission rates between hosts. Recently, Liu et al. [30] proposed a model that couples the evolutionary dynamics of viral virulence with the kinetics of transmission. A two-way coupling is achieved through the modeling method to study the influence of viral virulence evolution

dynamics on transmission dynamics. On the basis of this model, we consider the adaptive dynamic property of viral virulence development within the host to study the impact of mutant pathogens on the original system.

The remainder of this article is organized as follows. In Section 2, we develop an adaptive evolutionary model of viral virulence. In Section 3, we examine the existence and classification of equilibria and analyze their global stability. Furthermore, we explore the adaptive evolutionary dynamics of the system and investigate the influence of parameters on evolutionary singular strategies using both theoretical derivations and numerical simulations. Finally, in Section 4, the results are summarized and some discussion is provided.

2. The viral dynamics model

In general, the virus proliferates within the host cells of an infected individual, leading to the production of new virions that are subsequently released from the cell to infect additional susceptible cells. Upon entry into the host cells, the virus undergoes continuous replication and mutation, generating a variety of viral strains. This study considers a class of mathematical models that describe the interactions between susceptible cells and these diverse viral strains. Furthermore, free virions have a relatively short lifespan compared to infected cells, and it is assumed that viral load is positively correlated with the number of infected cells. The entire infection process is modeled as involving n viral strains and their corresponding n types of infected cells.

$x(t)$ denotes the number of uninfected target cells, while $y_j(t) \geq 0$ represents the number of cells infected by viral strain $j (j = 1, \ldots, n)$. The simplified model is presented below.

$$\begin{cases} \dfrac{\mathrm{d}x}{\mathrm{d}t} = \lambda - dx - \displaystyle\sum_{j=1}^{n} \beta_j(u_j) x y_j, \\ \dfrac{\mathrm{d}y_j}{\mathrm{d}t} = \beta_j(u_j) x y_j - a_j(u_j) y_j - q_j y_j. \end{cases} \tag{2.1}$$

In model (2.1), the production rate of uninfected cells is λ, and dx represents the natural mortality rate. The production rate of specifically infected cells by strain j is $\beta_j x y_j$, where mortality due to disease is represented by $a_j y_j$ and the natural mortality rate is $q_j y_j$. Here, β_j denotes the average probability that a target cell will be infected upon exposure to strain j. The term $1/(a_j + q_j)$ indicates the average duration that virus strain j remains in infected cells during the infection phase.

In this paper, we posit that the transmission rate and mortality rate attributable to virus j are directly linked to its virulence level, denoted as u_j. We model the costs and benefits associated with the development of specific traits in the virus by assuming that the functions $a_j(u_j)$ and $\beta_j(u_j)$ increase monotonically with increasing u_j (these are trade-off functions). The derivatives $a_j{}'(u_j)$ and $\beta_j{}'(u_j)$ reflect the extent to which virus j is constrained by cost and benefit considerations. If the virulence value of the virus is zero, it is assumed to be non-competitive and will consequently be eradicated. Therefore, we assume that $a_j(0) = \beta_j(0) = 0$. Moreover, due to limitations in susceptible cells and infected intracellular resources, viral transmission is finite, implying that $\beta_j(u_j)$ behaves as a saturation function. Additionally, we propose that increased virulence incurs higher costs due to resource

depletion, leading to a greater cost for higher virulence compared to lower virulence. Specifically, $\beta_j''(u_j) > 0$ for low virulence levels and $\beta_j''(u_j) < 0$ for high virulence levels. Based on these epidemiological considerations, we conclude that the functions $a_j(u_j)$ and $\beta_j(u_j)$ exhibit the following characteristics. Firstly, both $a_j(u_j)$ and $\beta_j(u_j)$ are non-negative for $u_j \geq 0$, with $a_j(0) = \beta_j(0) = 0$. Secondly, $a_j'(u_j)$ and $\beta_j'(u_j)$ are non-negative for $u_j \geq 0$, with $a_j'(0) = \beta_j'(0) = 0$. Thirdly, $\beta_j''(u_j) > 0$ for low virulence and $\beta_j''(u_j) < 0$ for high virulence.

We utilize a quantitative trait evolution model to simulate the evolutionary dynamics of the average virulence level u_j in a virus population [28, 34]. We hypothesize that virulence u_j can evolve, with its dynamics governed by the principles of quantitative genetics. As proposed by Iwasa et al. [28], the evolutionary dynamics of a single genotype, denoted as s, can be described by

$$\frac{\mathrm{d}s}{\mathrm{d}t} = G_{\tilde{s}} \frac{\mathrm{d}}{\mathrm{d}\tilde{s}} \ln W(\tilde{s}; s)\Big|_{\tilde{s}=s}. \tag{2.2}$$

This represents changes in the average genotype within the population s. In this equation, $W(\tilde{s}; s)$ denotes the fitness of an individual with genotype $\tilde{s}$ in a population with average genotype s. $G_{\tilde{s}}$ represents the additive genetic variance associated with genotype $\tilde{s}$.

Consequently, we formulate the evolutionary dynamics of virulence levels based on the virus dynamics model. Additionally, the additive genetic variance of u_j is represented by G_{u_j}. According to these assumptions, changes in the genotype u_j over a unit time interval can be described as follows,

$$\frac{\mathrm{d}u_j}{\mathrm{d}t} = G_{u_j} \frac{\mathrm{d}}{\mathrm{d}u_j} \left(\frac{1}{y_j} \frac{\mathrm{d}y_j}{\mathrm{d}t} \right). \tag{2.3}$$

In this equation, $(\mathrm{d}y_j/\mathrm{d}t)/y_j$ represents logarithms of virus fitness. According to the virus dynamics (2.1), the increase in the number of infected cells during a unit time interval can be represented by

$$\frac{\mathrm{d}y_j}{\mathrm{d}t} = (\beta_j(u_j)x - a_j(u_j) - q_j)y_j = \phi_j(u_j)y_j. \tag{2.4}$$

Then,

$$\phi_j(u_j) = \frac{1}{y_j} \frac{\mathrm{d}y_j}{\mathrm{d}t}, \tag{2.5}$$

and

$$\phi_j'(u_j) = \frac{\mathrm{d}}{\mathrm{d}u_j} \left(\frac{1}{y_j} \frac{\mathrm{d}y_j}{\mathrm{d}t} \right). \tag{2.6}$$

Hence,

$$\frac{\mathrm{d}u_j}{\mathrm{d}t} = G_{u_j}\phi_j'(u_j) = G_{u_j}(\beta_j'(u_j)x - a'(u_j)). \tag{2.7}$$

Based on the differential equations above, we describe the virus dynamics model

$$\begin{cases} \dfrac{\mathrm{d}x}{\mathrm{d}t} = \lambda - dx - \displaystyle\sum_{j=1}^{n} \beta_j(u_j)xy_j, \\ \dfrac{\mathrm{d}y_j}{\mathrm{d}t} = \beta_j(u_j)xy_j - a_j(u_j)y_j - q_jy_j, \\ \dfrac{\mathrm{d}u_j}{\mathrm{d}t} = G_{u_j}(\beta_j'(u_j)x - a'(u_j)). \end{cases} \tag{2.8}$$

Note that the selection of trade-off functions is not unique, and their precise quantification remains ambiguous and inadequately defined [15, 19]. Motivated by the observation that pathogen-induced burst mortality exhibits a monotonic increase with parasite proliferation, we select a quadratic nonlinear function $a_j(u_j) = p_j u_j^2$, where the positive constant p_j represents the baseline disease-induced mortality rate. Similarly, inspired by the Holling type III functional response, we choose $\beta_j(u_j) = r_j u_j^2/(1 + c_j u_j^2)$, with the positive constant r_j denoting the baseline transmission rate and c_j as a dimensionless non-negative constant. Direct verification confirms that the chosen functions $\beta_j(u_j)$ and $a_j(u_j)$ satisfy the three assumptions mentioned above.

Then, by calculating, we can obtain the following model

$$\begin{cases} \dfrac{\mathrm{d}x}{\mathrm{d}t} = \lambda - dx - \displaystyle\sum_{j=1}^{n} \frac{r_j u_j^2}{1 + c_j u_j^2} x y_j, \\ \dfrac{\mathrm{d}y_j}{\mathrm{d}t} = \dfrac{r_j u_j^2}{1 + c_j u_j^2} x y_j - p_j u_j^2 y_j - q_j y_j, \\ \dfrac{\mathrm{d}u_j}{\mathrm{d}t} = G_j \left(\dfrac{r_j u_j x}{(1 + c_j u_j^2)^2} - p_j u_j \right), \end{cases} \tag{2.9}$$

where $G_j = 2G_{u_j}$,

$$\frac{\mathrm{d}u_j}{\mathrm{d}t} = G_j \left(\frac{r_j u_j x}{(1 + c_j u_j^2)^2} - p_j u_j \right) \leq G_j \left(\frac{\lambda M}{d} - a_0 u_j \right). \tag{2.10}$$

By exploiting the comparison principle, we have

$$\lim_{t \to \infty} \sup u_j(t) \leq \frac{\lambda M}{a_0 d}. \tag{2.11}$$

Consider the region

$$D = \left\{ (x, y_j, u_j) \in \mathbb{R}_+^3 : x + y_j \leq \frac{\lambda}{d}, u_j \leq \frac{\lambda M}{a_0 d} \right\}. \tag{2.12}$$

It is demonstrated that all the solutions to system (2.9) that begin in D will continue to remain in D for all $t \geq 0$. Therefore, it can be concluded that D is positively invariant, making it adequate to solely examine solutions within D. It is consistently presumed that the initial points are situated in D.

3. Dynamics of the evolutionary system

3.1. Multistrain competition model

Assuming that the virus does not undergo any changes and therefore remains a constant value, we can deduce that $\beta_j(u_j) = \beta_j$ and $a_j(u_j) = a_j$, both of which represent positive constants. The initial two equations hold the ability to determine the dynamic properties of system (2.9). And we can obtain

$$\begin{cases} \dfrac{\mathrm{d}x}{\mathrm{d}t} = \lambda - dx - \displaystyle\sum_{j=1}^{n} \beta_j x y_j, \\ \dfrac{\mathrm{d}y_j}{\mathrm{d}t} = \beta_j x y_j - a_j y_j - q_j y_j. \end{cases} \tag{3.1}$$

In this section, we assume that $a_j = a, q_j = q$, and different diseases strains have different infectivity, i.e.

$$\beta_1 > \beta_2 > \cdots \beta_j > \cdots > \beta_n. \tag{3.2}$$

The following is the basic reproduction number R_j for the strain j, which is the average of new infections caused by any infected cell when all cells are healthy, with $\beta_j x$ representing the rate at which a single infected cell generates new infected cells. Since the average survival period of infected cells is $1/(a_j + q_j)$, it can be obtained

$$R_j = \frac{\lambda}{d} \frac{\beta_j}{a_j + q_j}. \tag{3.3}$$

The property of the isolated epidemic model is specifically determined by the reproduction number R_j. Combined with the previous condition (3.2), different strains have different basic reproduction numbers satisfying

$$R_1 > R_2 > \cdots R_j > \cdots > R_n. \tag{3.4}$$

Next, we analyze the dynamical properties of model (3.1). It is easy to find that there are two kinds of equilibria in system (3.1). First of all, one of these equilibria is the healthy equilibrium E_{10}, which means that all infected cell lines have disappeared, with $y_j = 0 (j = 1, \cdots, n)$, where the equilibrium is $E_{10} = (\lambda/d, 0, \cdots, 0)$. In this case, the number of healthy cells reaches its maximum. Secondly, the another one is the competitive equilibrium E_{11}, where only one strain of the virus exists in such an equilibrium state. Let the right end of the last n equations of system (3.1) equal to zero, which can be solved as $x^* = (a + q)/\beta_j$. Based on the assumption that different strains j have different β_j, then the value of $x(t)$ at the equilibrium can only be positively related to $(a + q)/\beta_j (j = 1, \cdots, n)$. It means that only the infected cells of strain j exist, and other infected cells do not exist, at this time

$$y_j^* = \frac{\lambda}{a + q} - \frac{d}{\beta_j} = \frac{d}{\beta_j} \left(R_j - 1 \right). \tag{3.5}$$

Therefore, for system (3.1), if there are $m (m \leq n)$ competing equilibria, the condition needs to be satisfied $R_j > 1 (j = 1, \cdots, m)$. At the same time, the m competitive equilibria can be expressed as

$$E_{1j} = \left(\frac{a + q}{\beta_j}, 0, \cdots, y_j^*, \cdots, 0 \right) (j = 1, \cdots, n). \tag{3.6}$$

The global stable property of system (3.1) can be obtained from the following theorem.

Theorem 3.1. *In condition (3.4), the healthy equilibrium $E_{10} = (\lambda/d, 0, \cdots, 0)$ of system (3.1) is globally asymptotically stable when $R_1 \leq 1$. In condition (3.4), the*

competition-equilibrium of system (3.1) is present if $R_1 > 1$ and the equilibrium E_{11} is globally asymptotically stable in case it exists, where

$$E_{11} = \left(\frac{a+q}{\beta_1}, \frac{\lambda}{a+q} - \frac{d}{\beta_1}, \cdots, 0\right) = \left(\frac{a+q}{\beta_1}, \frac{d}{\beta_1}\left(R_1 - 1\right), \cdots, 0\right). \tag{3.7}$$

Proof. Consider the Lyapunov function

$$V_{10}(x, \vec{y}) = x - x_0 - x_0 \ln \frac{x}{x_0} + \sum_{j=1}^{n} y_j, \tag{3.8}$$

which satisfies

$$\begin{aligned} V_0^{'}(x, \vec{y}) &= x' - \frac{x_0}{x}x' + \sum_{j=1}^{n} y_j^{'} \\ &= \frac{x - x_0}{x}x' + \sum_{j=1}^{n} y_j^{'} \\ &= \frac{x - x_0}{x}\left(\lambda - dx - \sum_{j=1}^{n}\beta_j x y_j\right) + \sum_{j=1}^{n}\left(\beta_j x y_j - a y_j\right) \\ &= -d \cdot \frac{x - x_0}{x}(x - \frac{\lambda}{d}) - (x - x_0)\sum_{j=1}^{n}\beta_j y_j + \sum_{j=1}^{n}\beta_j x y_j - \sum_{j=1}^{n} a y_j \\ &= -\frac{d}{x}(x - x_0)^2 + \frac{\lambda}{d}\sum_{j=1}^{n}\beta_j y_j - \sum_{j=1}^{n} a y_j \\ &= -\frac{d}{x}(x - x_0)^2 + \sum_{j=1}^{n} a(R_j - 1) y_j, \end{aligned} \tag{3.9}$$

where $V_0^{'}(x, \vec{y})$ is the total derivative of the solution curve along system (3.1) and $x_0 = \lambda/d$. From equation (3.4) and $R_j \leq 1$, we know that for all $j \geq 1$, $R_j - 1$ is constant negative. Obviously, $V_{10}^{'}(x, \vec{y}) \leq 0$ is always true if and only if $x = x_0, y_j = 0 (j = 1, \cdots, n)$ takes an equal sign. This leads to the conclusion that the healthy equilibrium E_{10} is globally asymptotically stable. When $R_1 = 1, V_{10}^{'} \leq 0$, $V_{10}^{'} = 0$ if and only if $x = x_0, y_j = 0 (j = 1, \cdots, n)$. Then in the set

$$\Omega = \left\{(x, \vec{y}) \in R_{\geq 0}^{n+1} \middle| x = x_0, y_j = 0 (j = 2, \cdots, n)\right\}, \tag{3.10}$$

the largest invariant set is E_{10}. Noting

$$x'|_{x=x_0} = \lambda - d x_0 - \sum_{j=1}^{n}\beta_j x_0 y_j = -\beta_1 x_0 y_1 = 0, \tag{3.11}$$

therefore,

$$y_1(t) \equiv 0. \tag{3.12}$$

According to LaSalle's invariance principle, E_{10} is globally asymptotically stable.

The following mainly discusses the case of $R_1 > 1$. Assuming that for all $R_j > 1$, there are n competitive equilibria $E_{11}, E_{12}, \cdots, E_{1n}$. In order to study the global state at E_{11}, we consider the function

$$V_{11}(x, \vec{y}) = x(t) - x^* - x^* \ln \frac{x(t)}{x^*} + y_j(t) - y_j^* - y_j^* \ln \frac{y_j(t)}{y_j^*} + \sum_{i=1, i\neq j}^{n} y_i(t), \quad (3.13)$$

where x^* and y_j^* are the numbers of susceptible and infected cells at the equilibrium E_{1j}. Calculate $V_{11}(x, \vec{y})$ along equation (3.1) solution for the derivative of the curve with respect to time t

$$\begin{aligned}
\frac{\mathrm{d}V_{11}}{\mathrm{d}t} =& (1 - \frac{x^*}{x})(\lambda - dx - \sum_{j=1}^{n} \beta_j x y_j) + (1 - \frac{y_j^*}{y_j})(\beta_j x y_j - a y_j - q y_j) \\
&+ \sum_{i=1, i\neq j}^{n} [\beta_i x y_i - (a+q) y_i] \\
=& - \frac{d}{x}(x - x^*)^2 + \sum_{j=1}^{n} \beta_j x^* y_j^* - \sum_{j=1}^{n} \beta_j x y_j - \sum_{j=1}^{n} \frac{\beta_j x^* x^* y_j^*}{x} + \sum_{j=1}^{n} \beta_j x^* y_j \\
&+ \beta_j x y_j - (a+q) y_j - \beta_j x y_j^* + (a+q) y_j^* + \sum_{i=1, i\neq j}^{n} \beta_i x y_i - \sum_{i=1, i\neq j}^{n} (a+q) y_i \\
=& - \frac{d}{x}(x - x^*)^2 + \beta_j x^* y_j^* (2 - \frac{x^*}{x} - \frac{x}{x^*}) + \sum_{i=1, i\neq j}^{n} (a+q) \left(\frac{R_i}{R_j} - 1 \right) y_i.
\end{aligned} \quad (3.14)$$

Obviously, the last two terms to the right of equation (3.14) are not positive. For all $i \neq j$ where $R_i < R_j$ holds, $E_{1j}$is globally asymptotically stable. Therefore, under the assumption of (3.4), we can conclude that E_{11} is globally asymptotically stable. □

Remark 3.1. The above results describe that even when n viruses strains infect target cells, only the strongest virus would survive. It also implies selection is applied in virus infection process. The above phenomenon is known as the "competitive exclusion principle". By biological meaning, in the virus competition process within host, only the viral strain with the maximum infectivity can win the competition, that is, be survival. The other strains go extinct.

3.2. The existence and local stability of the potential equilibria

By performing direct calculations, we determine that system (3.1) possesses a healthy equilibrium denoted as $E_{20}(x_0, 0, \cdots, 0, 0, \cdots, 0)$, along with a boundary equilibrium referred to as $E_{21}(\bar{x}, 0, \cdots, 0, \bar{u}_1, \cdots, \bar{u}_n)$. In the subsequent discussion, our primary focus will be directed towards examining the feasibility and local stability of the equilibria of system (2.9). Initially, we will analyze the existence of potential equilibria.

Theorem 3.2. *System (2.9) may possess a maximum of three equilibria, namely:*

(1) The equilibrium $E_{20}(x_0, 0, \cdots, 0, 0, \cdots, 0) = (\lambda/d, 0, \cdots, 0, 0, \cdots, 0)$ *is consistently present to denote absence of disease.*

(2) The boundary equilibrium E_{21} *exists if* $\lambda/d > \min\{p_j/r_j\}$*, where*

$$\begin{aligned} &E_{21}(\bar{x}, 0, \cdots, 0, \bar{u}_1, \cdots, \bar{u}_n) \\ &= \left(\frac{\lambda}{d}, 0, \cdots, 0, \left(\frac{\sqrt{\lambda r_1} - \sqrt{dp_1}}{c_1\sqrt{dp_1}}\right)^{\frac{1}{2}}, \cdots, \left(\frac{\sqrt{\lambda r_n} - \sqrt{dp_n}}{c_n\sqrt{dp_n}}\right)^{\frac{1}{2}}\right). \end{aligned} \tag{3.15}$$

(3) There may be n *possible scenarios for the positive equilibrium*

$$E_{2j} = \left(x^*, 0, \cdots, y_j^*, \cdots, 0, 0, \cdots, u_j^*, \cdots, 0\right)$$

if $\lambda/d > \min\{p_j/r_j\}$ *and* $R_{dj} > 1$*, and* j *is one of the values* $1, 2, \cdots, n-1$ *or* n*, where*

$$x^* = \frac{(\sqrt{p_j} + \sqrt{c_j q_j})^2}{r_j}, y_j^* = \frac{\sqrt{c_j}([r_j\lambda - d(\sqrt{p_j} + \sqrt{c_j q_j})^2])}{r_j(\sqrt{p_j q_j} + q_j\sqrt{c_j})},$$

$$u_j^* = \left(\frac{q}{a_0 c}\right)^{\frac{1}{4}}, R_{dj} = \frac{\sqrt{\lambda r_j p_j}(\sqrt{\lambda r_j} - \sqrt{dp_j})}{p_j\sqrt{d}(\sqrt{\lambda r_j} - \sqrt{dp_j}) + qc_j d\sqrt{p_j}}.$$

Take note that the threshold R_{dj} is determined by substituting the virulence u of R_j with the virulence at E_{21}, this infers that the threshold R_{dj} represents the basic reproduction number of the disease. Subsequently, we present findings concerning the local stability of equilibria.

The Jacobi matrix of system (2.9) at $E_{20}(x_0, 0, \cdots, 0, 0, \cdots, 0)$ $= (\lambda/d, 0, \cdots, 0, 0, \cdots, 0)$ is as follows

$$\begin{pmatrix} -d & 0 & \cdots & 0 & 0 & \cdots & 0 \\ 0 & -q_1 & \cdots & 0 & 0 & \cdots & 0 \\ \vdots & \vdots & & \vdots & \vdots & & \vdots \\ 0 & 0 & \cdots & -q_n & 0 & \cdots & 0 \\ 0 & 0 & \cdots & 0 & G_1(r_1x_0 - p_1) & \cdots & 0 \\ \vdots & \vdots & & \vdots & \vdots & & 0 \\ 0 & 0 & \cdots & 0 & 0 & \cdots & G_n(r_nx_0 - p_n) \end{pmatrix}. \tag{3.16}$$

Through straightforward calculation, it can be determined that the Jacobi matrix at E_{20} possesses $2n+1$ eigenvalues, including $-d, -q_1, \cdots, -q_n$, that are negative. Additionally, there exist other eigenvalues, which are $G_1(r_1x_0 - p_1), \cdots, G_n(r_nx_0 - p_n)$. When $\lambda/d > \min\{p_j/r_j\}$, E_{20} demonstrates instability. Conversely, E_{20} is locally asymptotically stable when $\lambda/d < \min\{p_j/r_j\}$. In an analogous manner, the Jacobi matrix evaluated at $E_{21}(\bar{x}, 0, \cdots, 0, \bar{u}_1, \cdots, \bar{u}_n)$ possesses one negative eigenvalue, namely $-d$ and $2n$ other eigenvalues

$$\begin{aligned} &\frac{r_1\bar{u}_1^2}{1 + c_1\bar{u}_1^2}\bar{x} - p_1\bar{u}_1^2 - q_1, \cdots, \frac{r_n\bar{u}_n^2}{1 + c_n\bar{u}_n^2}\bar{x} - p_n\bar{u}_n^2 - q_n, \\ &G_1\left[\frac{r_1 - 3r_1c_1\bar{u}_1^2}{(1 + c_1\bar{u}_1^2)^3}\bar{x} - p_1\right], \cdots, G_n\left[\frac{r_n - 3r_nc_n\bar{u}_n^2}{(1 + c_n\bar{u}_n^2)^3}\bar{x} - p_n\right]. \end{aligned} \tag{3.17}$$

If $\lambda/d > \min\{p_j/r_j\}$ and $R_d < 1$, it can be demonstrated with ease that E_{21} is locally asymptotically stable.

Theorem 3.3. *(1) If $\lambda/d < \min\{p_j/r_j\}$, the healthy equilibrium E_{20} is globally asymptotically stable in D.*

(2) If the conditions $\lambda/d > \min\{p_j/r_j\}$ and $R_{dj} < 1$ are satisfied, the boundary equilibrium E_{21} can be determined to be globally asymptotically stable in $D \setminus \{E_{20}\}$.

Proof. In order to demonstrate the global stability of $E_{20}(x_0, 0, \cdots, 0, 0, \cdots, 0)$, we analyze the subsequent Lyapunov function $V_{2j}(t, u_j) = y_j(t) + u_j(t)$. Differentiating $V_2(t, u_j)$ along the trajectories of (2.9) yields

$$\begin{aligned}\frac{\mathrm{d}V_{2j}}{\mathrm{d}t} &= \left(\frac{r_j u_j^2}{1+c_j u_j^2}x - p_j u_j^2 - q_j\right) y_j + G_j\left(\frac{r_j x}{(1+c_j u_j^2)^2} - p_j\right) u_j \\ &\le \left(\frac{r_j\lambda}{d}u_j^2 - p_j u_j^2\right) y_j + G_j\left(\frac{r_j\lambda}{d} - p_j\right) u_j \\ &= \frac{u_j^2 y_j}{d}(r_j\lambda - p_j d) + \frac{G_j u_j}{d}(r_j\lambda - p_j d) \\ &= \left(\frac{u_j^2 y_j}{d} + \frac{G_j u_j}{d}\right)(r_j\lambda - p_j d).\end{aligned} \tag{3.18}$$

Given that all parameters are positive, if $\lambda/d < \min\{p_j/r_j\}$, then $\mathrm{d}V_{2j}/\mathrm{d}t \le 0$ for all $y_j, u_j \ge 0$ with $\mathrm{d}V_{2j}/\mathrm{d}t = 0$ only $\lambda/d = \min\{p_j/r_j\}$. By applying the LaSalle's invariance principle, it can be concluded that $\lim\limits_{t\to\infty} y_j(t) = \lim\limits_{t\to\infty} u_j(t) = 0$. When these limits are brought into system (2.9), we obtain $\lim\limits_{t\to\infty} x(t) = \lambda/d$. Therefore, E_{20} serves as a global attractor of system (2.9) when $\lambda/d < \min\{p_j/r_j\}$.

In order to demonstrate the global stability of $E_{21}(\bar{x}, 0, \cdots, 0, \bar{u}_1, \cdots, \bar{u}_n)$, we examine the subsequent Lyapunov function $V_2(t, u_j) = y_j$. This function exhibits the subsequent property throughtout the system.

$$\begin{aligned}\frac{\mathrm{d}V_2(t,u_j)}{\mathrm{d}t} &= \left(\frac{r_j u_j^2}{1+c_j u_j^2}x - p_j u_j^2 - q_j\right) y_j \\ &= (p_j u_j^2 + q_j)\left[\frac{r_j u_j^2 x}{(1+c_j u_j^2)(p_j u_j^2 + q_j)} - 1\right] y_j \\ &\le (p_j u_j^2 + q_j)\left[\frac{\lambda r_j u_j^2}{d(1+c_j u_j^2)(p_j u_j^2 + q_j)} - 1\right] y_j.\end{aligned} \tag{3.19}$$

Let $M(u_j) = \frac{\mathrm{d}V_j(t,u_j)}{\mathrm{d}t}$ and $w(u_j) = \frac{\lambda r_j u_j^2}{d(1+c_j u_j^2)(p_j u_j^2+q_j)} - 1$. Hence, we can further obtain

$$\begin{aligned}M(u_j) &= \frac{\lambda r_j u_j^2}{d(1+c_j u_j^2)} - p_j u_j^2 - q_j \\ &= -\frac{p_j}{c_j}l - \frac{\lambda r_j}{c_j d}\frac{1}{l} + \frac{2p_j}{c_j},\end{aligned} \tag{3.20}$$

where $l = 1 + c_j u_j^2$. And because of $\frac{p_j}{c_j}l + \frac{\lambda r_j}{c_j d}\frac{1}{l} \ge 2\frac{1}{c_j}\sqrt{\frac{\lambda p_j r_j}{d}}$, we can yield that the equilibrium value $\bar{u}_j$ denotes the highest point of $M(u_j)$ within the domain D. At

the same time, we can obtain

$$l=\sqrt{\frac{\lambda r_j}{p_j d}}, t=\frac{\sqrt{\lambda r_j}-\sqrt{p_j d}}{c_j\sqrt{p_j d}}, u_j=\left(\frac{\sqrt{\lambda r_j}-\sqrt{p_j d}}{c_j\sqrt{p_j d}}\right)^{\frac{1}{2}}.$$

Note that $w(\bar{u}_j)=R_{dj}$, and $\mathrm{d}V_2(t,u_j)/\mathrm{d}t \le (p_j u_j^2+q_j)(R_{dj}-1)y_j$. Due to the boundary equilibrium E_{21} exists if $\lambda/d>\min\{p_j/r_j\}$, and if $R_{dj}<1$,we can obtain $\mathrm{d}V_2(t,u_j)/\mathrm{d}t\le 0$ for all $y_j(t)\ge 0$ and $\mathrm{d}V_2(t,u_j)/\mathrm{d}t=0$ only at $y_j(t)=0$. □

Lemma 3.1. *If the conditions $\lambda/d>\min\{p_j/r_j\}$ and $R_{dj}>1$ are satisfied, it can be inferred that there is a constant $m>0$ for which*

$$\lim_{t\to\infty}\inf x(t)>m, \lim_{t\to\infty}\inf y_j(t)>m, \lim_{t\to\infty}\inf u_j(t)>m$$

with the initial data $(x(0),y_j(0),u_j(0))\in \inf D$. Furthermore, it should be noted that the constant m remains unaffected by the specific initial data within the interior D.

In system (2.9), taking different values of n will result in different systems of differential equations. We can use the geometric approach that is based on the second additive compound matrix method to study the global stability of endemic equilibria in different systems and obtain the conditions for the global stability of endemic equilibria. We take the case of $n=1$ to obtain system (3.21) and obtain the conditions for the globally asymptotically stability of the endemic equilibrium in this system. In the following, we present findings on the global stability of the endemic equilibrium E^*.

$$\begin{cases}\dfrac{\mathrm{d}x}{\mathrm{d}t}=\lambda-dx-\dfrac{ru^2}{1+cu^2}xy,\\ \dfrac{\mathrm{d}y}{\mathrm{d}t}=\dfrac{ru^2}{1+cu^2}xy-pu^2y-qy,\\ \dfrac{\mathrm{d}u}{\mathrm{d}t}=G\left(\dfrac{rux}{(1+cu^2)^2}-pu\right).\end{cases}\tag{3.21}$$

Theorem 3.4. *Let it be assumed that the given conditions $\lambda/d>\min\{p_j/r_j\}$ and $R_{dj}>1$. Then, there exists a positive $\bar{c}$ and a positive value of $\bar{r}$ such that the unique endemic equilibrium E^* can be considered globally asymptotically stable within* $\inf D$*, as long as the conditions $c>\bar{c}$ and $r>\bar{r}$ are satisfied, where*

$$\bar{c}=\frac{1}{m^2}, \bar{r}=\max\left\{\frac{\lambda^3M^2(1+cm^2)}{a_0m}, \frac{2\lambda^2M^2}{m^3}+\frac{1}{m^3}(1+cm^2)(q-2d)\right\}.$$

Proof. In the subsequent sections, we utilize the geometric methodology, founded upon the second additive compound matrix to examine the global stability of the endemic equilibrium. The persistent uniformity of (3.21) within the confined set D is synonymous with the presence of a compact set K belonging to the interior of D that acts as an absorbent for (3.21). As stated by Theorem 3.5 of [29], all that remains is to substantiate the generalized Bendixson criterion

$$z=\lim_{t\to\infty}\sup\sup_{i_0\in K}\frac{1}{t}\int_0^t\mu(B(i(k,i_0)))dk<0.\tag{3.22}$$

By performing a precise calculation, the Jacobian matrix of the linearized system corresponding to the coupled model (3.21) can be derived

$$J = \begin{pmatrix} -\frac{ru^2}{1+cu^2}y - d & -\frac{ru^2}{1+cu^2}x & \frac{2ru}{(1+cu^2)^2}xy \\ \frac{ru^2}{1+cu^2}y & \frac{ru^2}{1+cu^2}x & \frac{2ru}{(1+cu^2)^2}xy - 2puy \\ \frac{Gru}{(1+cu^2)^2} & 0 & G\left(\frac{rx(1-3cu^2)}{(1+cu^2)^3} - p\right) \end{pmatrix},$$

and the corresponding second additive compound matrix $J^{[2]}$ is

$$J^{[2]} = \begin{pmatrix} \frac{\dot{y}}{y} - \beta(u)y - d & 2uy(\frac{rx}{(1+cu^2)^2} - p) & \frac{rx}{(1+cu^2)^2}xy \\ 0 & -\beta(u)y - d + G(\frac{rx(1-3cu^2)}{(1+cu^2)^3} - p) & -\beta(u)x \\ -\frac{Gru}{(1+cu^2)^2} & \beta(u)y & \frac{\dot{y}}{y} + G\left(\frac{rx(1-3cu^2)}{(1+cu^2)^3} - p\right) \end{pmatrix},$$

where the upper dot represents the derivative, $\frac{\mathrm{d}\triangle}{\mathrm{d}t}$. To begin, we establish the definition of A.

$$A(x, y, u) = \begin{pmatrix} \frac{1}{2} & 0 & 0 \\ 0 & \frac{x}{u} & 0 \\ 0 & \frac{x}{u} & \frac{x}{u} \end{pmatrix},$$

thus $A_f = (DA)(f)$. Namely, the matrix A_f is obtained by substituting each element a_{ij} in A with its directional derivative in the direction of vector field f, resulting in a_{ijf}. It is evident that A is nonsingular and C^1 in $intD$. The vector field of system (3.21) shall be denoted as f. Consequently, it can be deduced that

$$A_f = \begin{pmatrix} 0 & 0 & 0 \\ 0 & \frac{\dot{x}}{u} - \frac{x\dot{u}}{u^2} & 0 \\ 0 & \frac{\dot{x}}{u} - \frac{x\dot{u}}{u^2} & \frac{\dot{x}}{u} - \frac{x\dot{u}}{u^2} \end{pmatrix}, A^{-1} = \begin{pmatrix} 2 & 0 & 0 \\ 0 & \frac{u}{x} & 0 \\ 0 & -\frac{u}{x} & \frac{u}{x} \end{pmatrix}.$$

Furthermore,

$$A_f A^{-1} = \begin{pmatrix} 0 & 0 & 0 \\ 0 & \frac{\dot{x}}{x} - \frac{\dot{u}}{u} & 0 \\ 0 & 0 & \frac{\dot{x}}{x} - \frac{\dot{u}}{u} \end{pmatrix}.$$

The matrix $B = A_f A^{-1} + AJ^{[2]}A^{-1}$can be expressed in the subsequent block configuration

$$B = \begin{pmatrix} B_{11} & B_{12} \\ B_{21} & B_{22} \end{pmatrix}, B_{22} = \begin{pmatrix} b_{11} & b_{12} \\ b_{21} & b_{22} \end{pmatrix},$$

where

$$b_{11} = -\beta(u)y - d + G\left(\frac{rx(1-3cu^2)}{(1+cu^2)^3} - p\right) + \beta(u)x + \frac{\dot{x}}{x} - \frac{\dot{u}}{u},$$

$$
\begin{aligned}
b_{12} &= -\beta(u)x, \\
b_{21} &= a(u) + q - d, \\
b_{22} &= -\beta(u)x + \frac{\dot{y}}{y} + G\left(\frac{rx(1-3cu^2)}{(1+cu^2)^3} - p\right) + \frac{\dot{x}}{x} - \frac{\dot{u}}{u}.
\end{aligned}
$$

Let (i, j, k) represent the vectors in R^3 and the norm $|\cdot|$ in R^3 is selected as

$$|(i, j, k)| = \sup\{|i|, |j|, |k|\}.$$

In mathematical terms, the Lozinskii measure of B with respect to the induced matrix norm $|\cdot|$ in R^3, which is determined by a specific definition, can be denoted as $\mu(B)$, where

$$\mu(B) = \lim_{t \to 0^+} \frac{|y + \mu B| - 1}{h}.$$

The Lozinskil measure $\mu(B)$ in terms of $|\cdot|$ can be approximated through the following estimation.

$$\mu(B) \leq \sup\{g_1, g_2\},$$

where

$$g_1 = \mu_1(B_{11}) + |B_{12}|, g_2 = |B_{21}| + \mu_1(B_{22}).$$

The matrix norms denoted as $|B_{12}|$ and $|B_{21}|$ are related to the L_1 vector norm, while the symbol μ represents the Lozinskii measure in relation to the L_1 norm. To elaborate further,

$$\mu_1(B_{11}) = \frac{\dot{y}}{y} - \beta(u)y - d, |B_{12}| = \max\left\{\frac{a(u)}{x}y, \frac{ru^2}{(1+cu^2)^2}y\right\}, |B_{21}| = \frac{2Grx}{(1+cu^2)^2}.$$

In order to compute the value of $\mu_1(B_{22})$, it is necessary to add the absolute value of the off-diagonal elements to the diagonal element within each column of B_{22}. Subsequently, the larger value between the two resulting sums should be taken. As a result of this computation, we ultimately acquire the desired value.

$$
\begin{aligned}
\mu_1(B_{22}) =& G\left(\frac{rx(1-3cu^2)}{(1+cu^2)^3} - p\right) + \frac{\dot{x}}{x} - \frac{\dot{u}}{u} \\
&+ \max\left\{a(u) + \beta(u)x - \beta(u)y + q - 2d, \frac{\dot{y}}{y}\right\}.
\end{aligned}
$$

The overall representations of g_1 and g_2, pertaining to system (3.21), are consequently

$$g_1 = \mu_1(B_{11}) + |B_{12}| = \frac{\dot{y}}{y} - d + \max\left\{\frac{a(u)}{x}y - \beta(u)y, \frac{ru^2}{(1+cu^2)^2}y - \beta(u)y\right\}.$$

Since

$$\frac{ru^2}{(1+cu^2)^2}y - \beta(u)y = \frac{\beta(u)}{1+cu^2}y - \beta(u)y = \frac{-\beta(u)cu^2y}{1+cu^2},$$

it follows that

$$g_1 = \frac{\dot{y}}{y} - d + \max\left\{\frac{a(u)}{x}y - \beta(u)y, \frac{-\beta(u)cu^2y}{1+cu^2}\right\},$$

and

$$\begin{aligned} g_2 =& \frac{2Grx}{(1+cu^2)^2} + G\left(\frac{rx(1-3cu^2)}{(1+cu^2)^3} - p\right) \\ &+ \frac{\dot{x}}{x} - \frac{\dot{u}}{u} + \max\left\{a(u) + \beta(u)x - \beta(u)y + q - 2d, \frac{\dot{y}}{y}\right\}. \end{aligned}$$

Lemma 3.2. *There are positive constants m and T_1, which do not depend on $x(0)$ (the compact absorbing set), such that*

$$x(t) \geq m, y(t) \geq m, u(t) \geq m, t > T_1. \tag{3.23}$$

Furthermore, we shall delve into each case individually in the subsequent sections for a comprehensive analysis. The first case is $g_1 \geq g_2$, and the other case is $\mu(B) \leq g_1$.

In the first case, it can be deduced that $\mu(B) \leq g_1$. It should be noted that $\beta(u)$ and $a(u)$ are both strictly increasing functions for $u > 0$. Consequently, by considering these conditions, it can be inferred that

$$\mu(B) \leq \frac{\dot{y}}{y} - d + \max\left\{\frac{a(u)}{x}y - \beta(u)y, \frac{-\beta(u)cu^2y}{1+cu^2}\right\}.$$

Because of

$$\lim_{t\to\infty} u(t) \leq \frac{\lambda M}{a_0 d},$$

we have

$$\mu(B) \leq \frac{\dot{y}}{y} - d + \max\left\{\frac{a(\lambda\overline{W})}{md} - \beta(m)m, \frac{-\beta(u)cu^2y}{1+cu^2}\right\}, t > T_1,$$

where $\overline{W} = \frac{\lambda M}{a_0 d}$. Define $\widetilde{r}_1 = \frac{\lambda^3 M^2(1+cm^2)}{a_0 m}$. If $r_0 > \widetilde{r}_1$, then $\mu(B) \leq \frac{\dot{y}}{y} - d$ for $t > T_1$. For any $t > 0$, a solution $(x(t), y(t), u(t))$ exists for the combined system (3.21) when the initial values $(x(0), y(0), u(0))$ are within the absorbing set K. It is derived from the inequality $y(t) \leq \frac{\lambda}{d}$ for $\forall t \geq 0$ that there exists a $T_2 > 0$ such that $t > \max\{T_1, T_2\}$. Furthermore, when $r_0 > \widetilde{r}_1$, it can be concluded that

$$\frac{1}{t}\int_0^t \mu(B)dt \leq \frac{1}{t}\ln\frac{y(t)}{y(0)} - d \leq -\frac{d}{2}$$

holds for all $(x(0), y(0), u(0))$ within K. This, in turn, leads to $\tilde{z} \leq -\frac{d}{2} < 0$, and validates the generalized Bendixson criterion stated in equation (3.22) for case one.

For case two, we can obtain $\mu(B) \leq g_2$. Take note of the aforementioned system (3.21) that offers the subsequent equivalences

$$\frac{\dot{y}}{y} = \beta(u)x - a(u) - q, \frac{\dot{u}}{u} = G\left(\frac{rx}{(1+cu^2)^2} - p\right).$$

Hence, we have

$$g_2 = \frac{2Grx}{(1+cu^2)^2} + G\left(\frac{rx(1-3cu^2)}{(1+cu^2)^3} - p\right) + \frac{\dot{N}}{N} - \frac{\dot{u}}{u} + \max\left\{2a(u) - \beta(u)y + q - 2d, 0\right\}.$$

Furthermore, we can obtain

$$\mu(B) \leq \frac{\dot{N}}{N} + \frac{2Grx(1-cm^2)}{(1+cu^2)^3} + \max\left\{2a(\overline{W}) - \beta(m)m + q - 2d, 0\right\}, t > T_1,$$

where $\overline{W} = \frac{\lambda M}{a_0 d}$. Define

$$\bar{c} = \frac{1}{m^2}, \widetilde{r}_2 = \frac{2\lambda^2 M^2}{m^3} + \frac{1}{m^3}(1+cm^2)(q-2d).$$

Utilizing our selection of $\bar{c}$, $\widetilde{r}_2$ and (3.23), we deduce the existence of a constant $\bar{h} > 0$ whereby $\mu(B)$ is bounded by $\dot{N}/N - \bar{h}$ for $c > \bar{c}, \gamma > \widetilde{r}_2$ and $t > T_1$. Similarly, adhering to $N(t) \leq \lambda/d$ for $\forall t \geq 0$, in conjunction with any solution $(x(t), y(t), u(t))$ to (3.21), there exists $T_3 > 0$ such that for $(x(0), y(0), u(0)) \in Kc > \bar{c}, \gamma > \widetilde{r}_2$, and $t > \max\{T_1, T_3\}$, the inequality $\tilde{z} \leq -\bar{h}/2 < 0$ holds true. Consequently, the validity of the generalized Bendixson criterion stated in (3.22) is established in case two. □

In conclusion, it is understood that

$$c > \bar{c}, r > \max\left\{\widetilde{r}_1, \widetilde{r}_2\right\}.$$

Then it can be stated that

$$\tilde{z} \leq \min\left\{-\frac{d}{2}, -\frac{\bar{h}}{2}\right\} < 0, t > T_1, T_2, T_3.$$

As a result, the generalized Bendison criterion provided by equation (3.22) is confirmed. Based on Theorem 3.5, the parameters c and r may bear great importance in ensuring the overall stability of the endemic equilibrium.

3.3. The dynamical characteristics with the evolution of pathogen

In scenarios where the rate of evolutionary adaptation is exceptionally slow, the occurrence of mutant viruses and mutations in viral virulence is rare. By employing the adaptive dynamics approach, we argue that a mutant virus can invade and induce substitutions in virulence, which we rigorously demonstrate through detailed mathematical analysis. Notably, the basic reproduction number of the epidemic model (equation 2.8), denoted as $R_j(u_j)$, is given by $\frac{\lambda}{d}\frac{\beta_j(u_j)}{a_j(u_j)+q_j}$, under the assumption of no co-infection. According to Theorem 3.1, the endemic equilibrium E_{11} of the epidemic model is globally asymptotically stable when $R_j(u_j)$ exceeds one. Therefore, for the remainder of this section, we assume $R_j(u_j)$ surpasses one, implying that the mutant virus encounters the existing viral population at an endemic

equilibrium E_{11}. When a mutant virus with a slightly different level of infectiousness $\tilde{u}_j$ invades the existing viral population at low density, its invasion fitness can be quantified as follows,

$$f_j(u_j, \tilde{u}_j) = \beta_j(\tilde{u}_j)x^*(u_j) - a(\tilde{u}_j) - q_j.$$

If the value of $f_j(u_j, \tilde{u}_j)$ is greater than zero, it indicates that the population density of the mutant virus will increase, implying that the mutant virus has the ability to invade. Moreover, a successful invasion of the mutant virus will lead to a substitution of traits, where the resident population will become monomorphic again after a short period of epidemic transmission, but with a different trait. In the subsequent analysis, we will employ the method of Lyapunov function to establish a formal and rigorous proof of the statement that invasion results in trait substitution.

Theorem 3.5. *Assuming that the rate of evolutionary adaptation G_j is much smaller than 1, and the resident virulence u_j is significantly different from an evolutionarily singular strategy, it is possible to achieve a trait substitution if the invasion fitness for a mutant virus $f_j(\tilde{u}_j, u_j)$ is greater than 0.*

Proof. To begin, we enhance the existing epidemic model (2.1) by incorporating the existence of a population, denoted as y_{jm}, that is infected with a mutant virus possessing a virulence of $\tilde{u}_j$. When this mutant virus, characterized by a slightly altered virulence of $\tilde{u}_j$, infiltrates the resident populations at a limited density, the resultant dynamics of the resident-mutant epidemic can be described as follows.

$$\begin{cases} \dfrac{\mathrm{d}x}{\mathrm{d}t} = \lambda - dx - \displaystyle\sum_{j=1}^{n} \Big[\beta_j(u_j)xy_j + \beta_j(\tilde{u}_j)xy_{jm}\Big], \\ \dfrac{\mathrm{d}y_j}{\mathrm{d}t} = \beta_j(u_j)xy_j - a_j(u_j)y_j - q_j y_j, \\ \dfrac{\mathrm{d}y_{jm}}{\mathrm{d}t} = \beta_{jm}(\tilde{u}_j)xy_{jm} - a_j(\tilde{u}_j)y_{jm} - q_j y_{jm}, \end{cases} \tag{3.24}$$

where y_{jm} denotes the number of y_j-infected mutants at time t. For simplicity, let $\beta_j = \beta_j(u_j)$, $a_j(u_j) = a_j$,$\beta_{jm}(\tilde{u}_j) = \beta_{jm}$,$a_j(\tilde{u}_j) = a_{jm}$. Then, we can further obtain equation (3.25). And a boundary equilibrium of the simplified resident-mutant epidemic model (3.25) can be represented as $(x^*, 0, \cdots, 0, 0, \cdots, y^*_{jm}, \cdots, 0)$.

$$\begin{cases} \dfrac{\mathrm{d}x}{\mathrm{d}t} = \lambda - dx - \displaystyle\sum_{j=1}^{n} \Big[\beta_j xy_j + \beta_{jm}xy_{jm}\Big], \\ \dfrac{\mathrm{d}y_j}{\mathrm{d}t} = \beta_j xy_j - a_j y_j - q_j y_j, \\ \dfrac{\mathrm{d}y_{jm}}{\mathrm{d}t} = \beta_{jm}xy_{jm} - a_{jm}y_{jm} - q_j y_{jm}. \end{cases} \tag{3.25}$$

Subsequently, employing the Lyapunov function methodology, it is demonstrated that if the magnitude of the difference between $\tilde{u}_j$ and u_j is adequately small, u_j does not exist in the vicinity of the singularity, and $f_j(u_j, \tilde{u}_j)$ exceeds zero, the boundary equilibrium $(x^*, 0, \cdots, 0, 0, \cdots, y_{jm}, \cdots, 0)$ is globally asymptotically stable within the domain $\Lambda = \{x > 0, y_j \geq 0, y_{jm} > 0\}, j = 1, \cdots, n$. Consequently, this implies that the emergence of a mutant virus through a victorious invasion leads to the substitution of traits.

We can define the following Lyapunov function

$$V_m = V_1 + V_2 + V_3, \tag{3.26}$$

where

$$\begin{aligned} V_1 &= x - x^* - x^* \ln \frac{x}{x^*}, \\ V_2 &= \sum_{j=1}^{n} y_j, \\ V_3 &= \sum_{j=1}^{n} \left(y_{jm} - y_{jm}^* - y_{jm}^* \ln \frac{y_{jm}}{y_{jm}^*} \right). \end{aligned} \tag{3.27}$$

By constructing the aforementioned Lyapunov function and employing a similar calculation method, we omit the detailed calculation steps. The following conclusions can be drawn: Given that $f_j(\tilde{u}_j, u_j)$ is greater than zero when the absolute difference between $\tilde{u}_j$ and u_j is sufficiently small, and provided that u_j is not in close proximity to the singularity, the global asymptotic stability of the equilibrium $(x^*, 0, \cdots, 0, 0, \cdots, y_{jm}^*, \cdots, 0)$ can be established using the Lyapunov-LaSalle invariance principle. This conclusion completes the proof. □

Numerical simulations can further verify these conclusions. Specifically, for $n = 3$, we observe the dynamics of three viruses and their mutated forms.

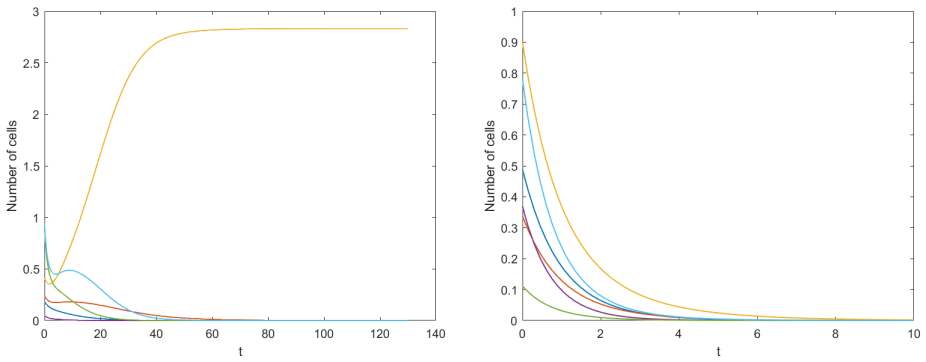

(a) (b)

Figure 1. When $n = 3$, the number of resident viruses and mutant viruses changes with time t. (a) Plot of the viral load of the six viruses in the presence of $R_j > 1$ as a function of time t. (b) Plot of the viral load of the six viruses as a function of time t when all $R_j < 1$.

From Figure 1(a), it is evident that as time progresses, only one type of infected cell maintains a stable load value while others tend to zero. Only the equilibrium with maximum characteristics is globally asymptotically stable. For the case where every strain has different basic reproductive number from each other, the coexistence of different strains is impossible. From Figure 1(b), it is clear that when all basic reproduction number R_j are less than one, the number of infected cells tends to zero, confirming the theoretical findings.

The viral virulence will undergo gradual evolution via repeated invasion and replacement. The evolutionary direction of this change is dictated by the selection

gradient $g(u_j)$'s sign, as indicated by

$$g(u_j) = \frac{\partial f_j(\tilde{u}_j, u_j)}{\partial \tilde{u}_j}\bigg|_{\tilde{u}_j = u_j} = \beta_j'(u_j)x^*(u_j) - a'(u_j). \tag{3.28}$$

An evolutionarily singular strategy refers to a strategy u_j^* for which the selection gradient $g(u_j)$ becomes zero. In the case that $R_j(u_j)$ is greater than one and the epidemic equilibrium is globally asymptotically stable, the equilibrium level can be utilized as a representative level for the long-term epidemic dynamics. In this context, the evolutionary dynamic is estimated through averaged dynamics using the following approach

$$\frac{\mathrm{d}u_j}{\mathrm{d}t} = G_{u_j}(\beta_j{}'(u_j)x^*(u_j) - a'(u_j)),$$

where

$$x^*(u_j) = \frac{a_j(u_j) + q_j}{\beta_j} = \left(p_j u_j^2 + q_j\right)\frac{1 + c_j u_j^2}{r_j u_j^2}.$$

Hence,

$$\begin{aligned} \frac{\mathrm{d}u_j}{\mathrm{d}t} &= G_{u_j}\left(\beta_j'(u_j)x^*(u_j) - a'(u_j)\right) \\ &= 2G_{u_j}\left(\frac{p_j u_j^2 + q_j}{u_j(1 + c_j u_j^2)} - p_j u_j\right). \end{aligned} \tag{3.29}$$

The result of algebraic calculation indicates that system (3.29) possesses a distinctive equilibrium, u_j^*, given by the equation $(q_j/p_j c_j)^{\frac{1}{4}}$. Based on equation (3.28), it can be concluded that the exclusive equilibrium u_j^* represents the only evolutionarily singular strategy. Furthermore, the negative eigenvalue of the Jacobian matrix at u_j^* suggests that u_j^* is globally asymptotically stable, and the singular strategy u_j^* demonstrates convergence stability. In other words, if a population having a neighboring strategy is invaded by a mutant virus that is even more proximate to u_j^*, since

$$\frac{\partial^2 f_j(\tilde{u}_j, u_j)}{\partial \tilde{u}_j^2}\bigg|_{\tilde{u}_j = u_j = u_j^*} = \beta_j''(u_j)x^*(u_j) - a''(u_j)\big|_{u_j = u_j^*} < 0, \tag{3.30}$$

the strategy u_j^* is considered to be evolutionarily stable as it cannot be invaded by any nearby mutants. Consequently, u_j^* is regarded as a continuously stable strategy(CSS) and signifies the ultimate outcome of the evolutionary process. Additionally, the summarized findings regarding the existence and stability of the averaged system (3.29) are presented below.

Theorem 3.6. *When $R_j(u_j)$ exceeds 1, the positive equilibrium u_j^* of equation (3.29) demonstrates global asymptotic stability and serves as the continuously stable strategy(CSS).*

To verify the above conclusions, we try to draw a pairwise invasibility plot(PIP). The selected parameters are $c_j = 0.2, q_j = 0.1, p_j = 0.2, r_j = 0.5$. The evolutionary singularity strategy u_j^* is the intersection of the fitness function $f_j(\tilde{u}_j, u_j)$ and the diagonal $\tilde{u}_j = u_j$. Since convergent stability and evolutionary stability are two separate characteristics, evolutionary singular strategies can be divided into

four categories. By observing the pairwise invasion graph, we can know which of the evolutionary singular strategies under this parameter condition belongs to, and which is used to verify the conclusions obtained above. From Figure 2, we can see that the evolutionary singular strategy does the perpendicular line in its upper and lower neighborhoods, and the perpendicular line falls in the region of $f_j(\tilde{u_j}, u_j) < 0$ in the white part, so the singular strategy u_j^* corresponding to this point is evolutionarily stable. We hereby present the findings resulting from the integration of the transmission rate β_j, which is dependent on virulence, with the mortality caused by illness $a_j(u_j)$, utilizing the identical parameter values as displayed in Figure 3(a). For the transmission rate, we have opted for $\beta_j(u_j) = \frac{r_j u_j^2}{1+c_j u_j^2}$, while for the mortality rate, we have selected $a_j(u_j) = p_j u_j^2$. As we can see in Figure 3(b), $u_j(t)$ increases gradually as t increases, and when t reaches a certain value, $u_j(t)$ stabilizes at a fixed value. And the initial value $u_j(0) = 1$.

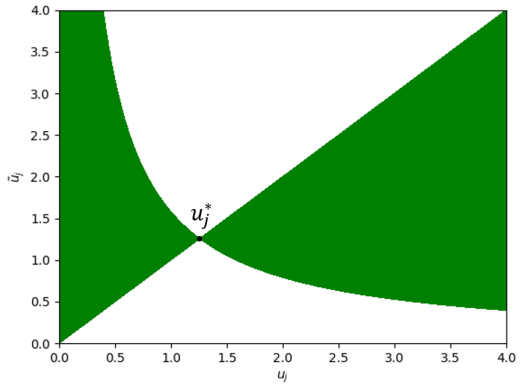

Figure 2. Continuously stable strategy of pathogen virulence. The green part of the graph represents the invasion fitness function $f_j(u_j, \tilde{u}_j) > 0$, and the white part represents the invasion fitness function $f_j(u_j, \tilde{u}_j) < 0$.

In the subsequent analysis, our aim is to demonstrate that the CSS virulence significantly enhances the basic reproduction number of a rare mutant. It should be noted that the basic reproduction number of the epidemic model is denoted as $R_0[\tilde{u}_j, u_j]$. Let us consider a scenario where a rare mutant with a virulence level represented by $\tilde{u}_j$ successfully infiltrates a population of resident parasites with a virulence level of u_j. The formula representing the fitness of the mutant, as explained in reference [20], can be expressed as follows

$$R_0[\tilde{u}_j, u_j] = \frac{\lambda}{d} \frac{\beta_j(\tilde{u}_j)}{a_j(\tilde{u}_j) + q_j}.$$

We then proceed to demonstrate that the strategy $\tilde{u}_j$ maximizes the basic reproduction number $R_0[\tilde{u}_j, u_j]$ when $\tilde{u}_j$ equals u_j. By taking the derivative of $R_0[\tilde{u}_j, u_j]$, we obtain the following result

$$\frac{\mathrm{d}R_0[\tilde{u}_j, u_j]}{\mathrm{d}\tilde{u}_j}\Big|_{\tilde{u}_j = u_j} = \frac{\lambda}{d} \frac{2r_j \tilde{u}_j (q_j - c_j p_j \tilde{u}_j^4)}{(p_j \tilde{u}_j^2 + q_j)^2 (1 + c_j \tilde{u}_j^2)^2}.$$

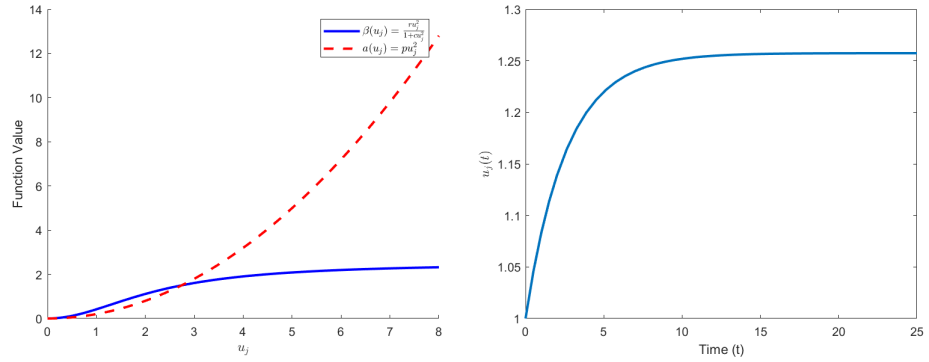

(a) (b)

Figure 3. (a) The function plots of transmission rate and mortality due to illness as a function of viral virulence. (b) The change of viral virulence over time.

Thus, it can be deduced that the derivative of $R_0[\tilde{u}_j, u_j]$ with respect to $\tilde{u}_j$, evaluated at $\tilde{u}_j = u_j$, is equal to zero only when $\tilde{u}_j$ equals u_j^*, thereby establishing that u_j^* represents the highest point of value for $R_0[\tilde{u}_j, u_j]$.

Overall, it can be concluded that the globally asymptotically stable equilibrium (as demonstrated in Theorem 3.6) represents the state of continuous stability regarding virulence, which, in turn, maximizes the basic reproduction number $R_0[\tilde{u}_j, u_j]$ (depicted in Figures 4(a) and 4(b)).

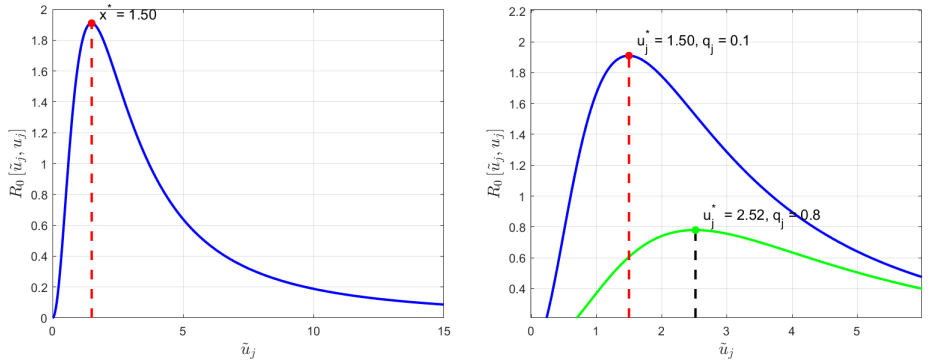

(a) (b)

Figure 4. The reproduction number of an rare mutant, denoted as $R_0[\tilde{u}_j, u_j]$, is compared to the virulence of mutant, represented as $\tilde{u}_j$. (a) The reproduction number in relation to the level of virulence associated with a particular strain, under the presumption of no direct reliance on other factors. (b) The alteration in continuously alongside a specified parameter, denoted as y, here we take y to q_j as an example.

3.4. Sensitivity analysis of continuously stable strategy(CSS)

In this section, we discuss how a continuously stable strategy of a virus may occur independently of the trade-off function by using the method of implicit differentiation, and how changes in the relevant statistical parameters of the virus affect the evolutionary behavior of virulence traits in pathogens.

First, we consider the effect of the intensity of the natural mortality rate q of infected cells on the continuously stable strategy(CSS). The determination of this can be attained through noticing the sign of the derivative of $\tilde{u}_j$ concerning q. To achieve this, we rely on the selection gradient $g(u_j^*, q)$ in equation (3.28) and carry out implicit differentiation of the equation $g(u_j^*, q) = 0$ with respect to q, while considering u_j^* as a function of q. Consequently, we obtain

$$\frac{\partial}{\partial q} g\left(u_j^*, q\right) = \left.\frac{\partial g(u_j, \tilde{u}_j)}{\partial u_j}\right|_{u_j=u_j^*} \frac{\mathrm{d}u_j^*}{\mathrm{d}q} + \left.\frac{\partial g(u_j, \tilde{u}_j)}{\partial q}\right|_{\tilde{u}_j=u_j^*} = 0. \tag{3.31}$$

By employing the defined expression of $g(u_j, q) = 0$, we proceed to rephrase equation (3.31) as

$$\frac{\mathrm{d}u_j^*}{\mathrm{d}q} = -\left(\frac{\partial}{\partial q}\left(\left.\frac{\partial f_j(\tilde{u}_j, u_j)}{\partial \tilde{u}_j}\right|_{\tilde{u}_j=u_j}\right)\right)_{u_j=u_j^*} \Bigg/ \left(\frac{\partial}{\partial u_j}\left(\left.\frac{\partial f_j(\tilde{u}_j, u_j)}{\partial \tilde{u}_j}\right|_{\tilde{u}_j=u_j}\right)\right)_{u_j=u_j^*}. \tag{3.32}$$

Due to its characteristic of convergence stability, denoted as "CSS", it can be implied that the denominator in equation (3.32) will consistently exhibit negativity. Thus, the sign of the derivative $\frac{\mathrm{d}u_j^*}{\mathrm{d}q}$ can be ascertained based on the numerator of equation (3.32). Through straightforward computations, the numerator of equation (3.32) can be derived as

$$\begin{aligned}\frac{\partial}{\partial q}\left(\left.\frac{\partial f_j(u_j, \tilde{u}_j)}{\partial \tilde{u}_j}\right|_{\tilde{u}_j=u_j}\right)_{u_j=u_j^*} &= \frac{\partial}{\partial q}\left(\beta_j'(u_j)x^*(u_j) - a'(u_j)\right)_{u_j=u_j^*} \\ &= \frac{\partial}{\partial q}\left(\beta_j'(u_j)\frac{a(u_j)+q}{\beta_j(u_j)} - a'(u_j)\right)_{u_j=u_j^*} \\ &= \frac{\beta_j'(u_j)}{\beta_j(u_j)} = \frac{2}{u_j(1+c_j u_j^2)},\end{aligned} \tag{3.33}$$

which is always positive. Therefore, for the Continuous Stable Strategy(CSS), $\frac{\mathrm{d}u_j^*}{\mathrm{d}q} > 0$ is always true, i.e., the evolutionary singular strategy u_j^* always increases with the parameter q. This result can be represented visually, as shown in Figure 5(a). This means that under the conditions of a given viral infectivity rate $\beta_j(u_j) = \frac{r_j u_j^2}{1+c_j u_j^2}$ and mortality due to disease $a_j(u_j) = p_j u_j^2$, if the intensity of the natural mortality rate q becomes stronger, the infection rate of normal cells will increase (because the virulence trait u_j will increase), and the whole system will develop in the direction of high infection rate and high mortality due to disease. Using the same analysis method, we obtain that the evolutionary singular strategy is monotonically decreasing with respect to parameters c and p, as shown in Figures 5(b) and 5(c).

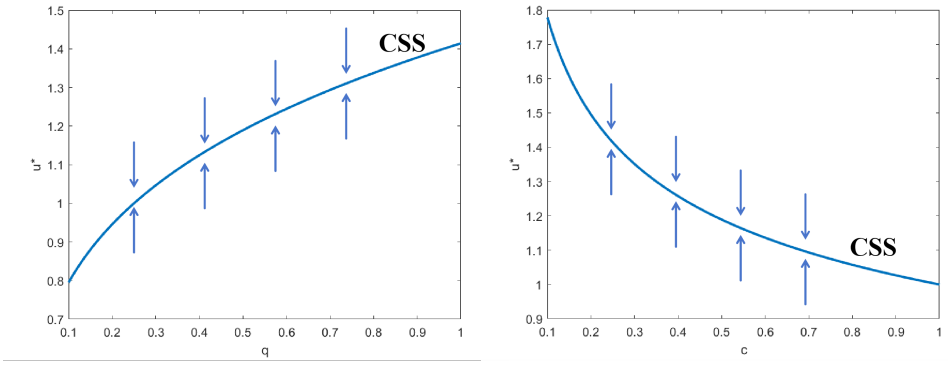

Figure 5. Diagram illustrating the evolutionary dynamics under varying parameter conditions. (a) Evolutionarily singular strategy u_j^* versus the natural death rate of infected cell q. (b) Evolutionarily singular strategy u_j^* versus parameter c in the trade-off function q. (c) Evolutionarily singular strategy u_j^* versus mortality due to disease p.

4. Discussion and conclusions

Understanding the evolutionary dynamics of virulence traits from a microscopic perspective is of great significance for the prevention and control of viral mutations. In this paper, we investigate the evolutionary dynamics of virulence traits in healthy cells transitioning to pathogen infection using the method of adaptive dynamics, based on a viral dynamics model of multiple infectious strains within the human body. Considering a viral evolutionary model with multiple virus strains, healthy cells can be infected by n distinct classes of viruses, which can mutate into strains with altered virulence traits compared to the original virus. Therefore, the stability conditions of the equilibrium of the original system and the parameters influencing the convergence or evolutionary stability strategy are crucial under such complex changes.

When we consider a scenario where virus evolution is ignored, i.e., the infection rate of healthy cells and the mortality rate of infected cells are constant parameters.

By using Lyapunov approaches, only equilibrium state E_{11} is shown to be globally asymptotically stable, which means only one strain with the maximum number can be survived. This also verifies and expands upon the competitive exclusion principle in [5]. Viral evolution tends to maximize the basic reproductive number.

When considering the evolution of the virus, we hypothesize that only traits associated with viral virulence can evolve adaptively, specifically the infection rate of viruses in healthy cells and the mortality rate of infected cells due to disease (trade-off functions) [2, 31]. Notably, the presence of multiple strains enables us to construct standard Lyapunov functions, thereby demonstrating the global asymptotic stability of the equilibrium. We examine the evolutionary trajectory of viral virulence traits from the perspective of adaptation dynamics. Furthermore, the sign of the invasion fitness function can be used to determine whether a mutant can invade and replace the resident virus. A Lyapunov function is constructed to demonstrate that such an invasion will result in trait replacement. The level of virulence traits obtained by selecting a gradient of zero is termed the evolutionary singular strategy. The type of ESS is determined by evaluating the second-order partial derivative of the invasion fitness function. It is proven that when the basic reproduction number exceeds one, the virulence level constitutes a globally asymptotically stable and continuously stable strategy. This conclusion is corroborated through pairwise invasion plots. Subsequently, sensitivity analysis of the CSS is conducted, revealing how other parameters influence the determination of the CSS. We observe that the continuously stable strategy increases with higher natural mortality rates of infected cells, decreases with increasing coefficients of the mortality function of infected cells, and diminishes as parameter c in the infection rate function rises.

References

[1] J.B. Alimonti, T.B. Ball and K.R. Fowke, *Mechanisms of CD4+ T lymphocyte cell death in human immunodeficiency virus infection and AIDS*, Journal of General Virology, 2003, 84(7): 1649–1661.

[2] S. Alizon, A. Hurford, N. Mideo and M. Van Baalen, *Virulence evolution and the trade-off hypothesis: history, current state of affairs and the future*, Journal of Evolutionary Biology, 2009, 22(2): 245–259.

[3] H.K. Altes, D. Wodarz and V.A.A. Jansen, *The dual role of CD4 T helper cells in the infection dynamics of HIV and their importance for vaccination*, Journal of Theoretical Biology, 2002, 214(4): 633–646.

[4] J. Antonovics and P. Thrall, *The cost of resistance and the maintenance of genetic polymorphism in host-pathogen systems*, Proceedings of the Royal Society of London. Series B: Biological Sciences, 1994, 257(1349): 105–110.

[5] M. Begon and C.R. Townsend, *Ecology: from individuals to ecosystems*, John Wiley and Sons, 2020.

[6] A. Best, H. Tidbury, A. White and M. Boots, *The evolutionary dynamics of within-generation immune priming in invertebrate hosts*, Journal of the Royal Society Interface, 2013, 10(80): 20120887.

[7] A. Best, A. White and M. Boots, *The implications of coevolutionary dynamics to host-parasite interactions*, The American Naturalist, 2009, 173(6): 779–791.

[8] A. Best, A. White and M. Boots, *The evolution of host defence when parasites impact reproduction*, Evolutionary Ecology Research, 2017, 18: 393–409.

[9] B. Bittner, S. Bonhoeffer and M.A. Nowak, *Virus load and antigenic diversity*, Bulletin of Mathematical Biology, 1997, 59(5): 881–896.

[10] M. Bonds, *Host life-history strategy explains pathogen-induced sterility*, The American Naturalist, 2006, 168(3): 281–293.

[11] M. Boots, A. Best, M. R. Miller and A. White, *The role of ecological feedbacks in the evolution of host defence: what does theory tell us?* Philosophical Transactions of the Royal Society B: Biological Sciences, 2009, 364(1513): 27–36.

[12] O.J. Cohen and A.S. Fauci, *Transmission of multidrug-resistant human immunodeficiency virus-the wake-up call*, New England Journal of Medicine, 1998, 339(5): 341–343.

[13] D. Coombs, M.A. Gilchrist and C.L. Ball, *Evaluating the importance of within- and between-host selection pressures on the evolution of chronic pathogens*, Theoretical Population Biology, 2007, 72(4): 576–591.

[14] R.J. de Boer and M.C. Boerlijst, *Diversity and virulence thresholds in AIDS*, Proceedings of the National Academy of Sciences, 1994, 91(2): 544–548.

[15] J.H.P. Dawes and M.O. Souza, *A derivation of Holling's type I, II and III functional responses in predator-prey systems*, Journal of Theoretical Biology, 2013, 327: 11–22.

[16] Z. Feng, X. Cen, Y. Zhao and J.X. Velasco-Hernandez, *Coupled within-host and between-host dynamics and evolution of virulence*, Mathematical Biosciences, 2015, 270: 204–212.

[17] A.P. Galvani, *The role of mutation accumulation in HIV progression*, Proceedings of the Royal Society B: Biological Sciences, 2005, 272(1574): 1851–1858.

[18] J. Gamberg and M. Grant, *Cytotoxic T lymphocytes in human immunodeficiency virus type-1 infection important or impotent?* Clinical and Applied Immunology Reviews, 2000, 1(1): 17–36.

[19] S. Gandon, T. Day, C.J.E. Metcalf and B.T. Grenfell, *Forecasting epidemiological and evolutionary dynamics of infectious diseases*, Trends in Ecology and Evolution, 2016, 31(10): 776–788.

[20] S. Gandon, M.J. Mackinnon, S. Nee and A.F. Read, *Imperfect vaccines and the evolution of pathogen virulence*, Nature, 2001, 414(6865): 751–756.

[21] M.A. Gilchrist and D. Coombs, *Evolution of virulence: interdependence, constraints, and selection using nested models*, Theoretical Population Biology, 2006, 69(2): 145–153.

[22] A.N. Gorban, *Selection theorem for systems with inheritance*, Mathematical Modelling of Natural Phenomena, 2007, 2(4): 1–45.

[23] D.D. Ho, A.U. Neumann, A.S. Perelson, W. Chen, J.M. Leonard and M. Markowitz, *Rapid turnover of plasma virions and CD4 lymphocytes in HIV-1 infection*, Nature, 1995, 373(6510): 123–126.

[24] E.C. Holmes, L.Q. Zhang, P. Simmonds, C.A. Ludlam and A.J. Brown, *Convergent and divergent sequence evolution in the surface envelope glycoprotein of human immunodeficiency virus type 1 within a single infected patient*, Proceedings of the National Academy of Sciences, 1992, 89(11): 4835–4839.

[25] G. Huang, Y. Takeuchi and A. Korobeinikov, *HIV evolution and progression of the infection to AIDS*, Journal of Theoretical Biology, 2012, 307: 149–159.

[26] Y. Iwasa, F. Michor and M. Nowak, *Some basic properties of immune selection*, Journal of Theoretical Biology, 2004, 229(2): 179–188.

[27] Y. Iwasa, F. Michor and M.A. Nowak, *Virus evolution within patients increases pathogenicity*, Journal of Theoretical Biology, 2005, 232(1): 17–26.

[28] Y. Iwasa, A. Pomiankowski and S. Nee, *The evolution of costly mate preferences II. The "handicap" principle*, Evolution, 1991, 45(6): 1431–1442.

[29] M.Y. Li and J.S. Muldowney, *A geometric approach to global-stability problems*, SIAM Journal on Mathematical Analysis, 1996, 27(4): 1070–1083.

[30] Q. Liu and Y. Xiao, *A coupled evolutionary model of the viral virulence in an SIS community*, Discrete and Continuous Dynamical Systems-B, 2023, 28(9): 5012–5036.

[31] H. MacDonald, E. Akçay and D. Brisson, *Host phenology can drive the evolution of intermediate virulence strategies in some obligate-killer parasites*, Evolution, 2022, 76(6): 1183–1194.

[32] R. Medzhitov, *Recognition of microorganisms and activation of the immune response*, Nature, 2007, 449(7164): 819–826.

[33] D. Moskophidis, M. Battegay, M. van den Broek, E. Laine, U. Hoffmann-Rohrer and R.M. Zinkernagel, *Role of virus and host variables in virus persistence or immunopathological disease caused by a non-cytolytic virus*, Journal of General Virology, 1995, 76(2): 381–391.

[34] A. Mougi and Y. Iwasa, *Evolution towards oscillation or stability in a predator-prey system*, Proceedings of the Royal Society B: Biological Sciences, 2010, 277(1697): 3163–3171.

[35] M.A. Nowak and C.R.M. Bangham, *Population dynamics of immune responses to persistent viruses*, Science, 1996, 272(5258): 74–79.

[36] M.A. Nowak, R.M. May and K. Sigmund, *Immune responses against multiple epitopes*, Journal of Theoretical Biology, 1995, 175(3): 325–353.

[37] A.S. Perelson, A.U. Neumann, M. Markowitz, J.M. Leonard and D.D. Ho, *HIV-1 dynamics in vivo: virion clearance rate, infected cell life-span, and viral generation time*, Science, 1996, 271(5255): 1582–1586.

[38] A. Peschel and H.G. Sahl, *The co-evolution of host cationic antimicrobial peptides and microbial resistance*, Nature Reviews Microbiology, 2006, 4(7): 529–539.

[39] A. Rambaut, D. Posada, K.A. Crandall and E.C. Holmes, *The causes and consequences of HIV evolution*, Nature Reviews Genetics, 2004, 5(1): 52–61.

[40] R.M. Ribeiro, H. Mohri, D.D. Ho and A.S. Perelson, *In vivo dynamics of T cell activation, proliferation, and death in HIV-1 infection: why are CD4+ but not CD8+ T cells depleted?* Proceedings of the National Academy of Sciences, 2002, 99(24): 15572–15577.

[41] A. Theodosopoulos, A. Hund and S. Taylor, *Parasites and host species barriers in animal hybrid zones*, Trends in Ecology and Evolution, 2019, 34(1): 19–30.

[42] X. Wang, S. Wang, J. Wang and L. Rong, *A multiscale model of COVID-19 dynamics*, Bulletin of Mathematical Biology, 2022, 84(9): 99.